



Cite this: *RSC Adv.*, 2019, 9, 30007

# Rutin-modified silver nanoparticles as a chromogenic probe for the selective detection of Fe<sup>3+</sup> in aqueous medium†

Mayra S. Coutinho,<sup>a</sup> Eloah Latocheski,<sup>b</sup> Jannyely M. Neri,<sup>a</sup> Ana C. O. Neves,<sup>a</sup> Josiel B. Domingos,<sup>b</sup> Lívia N. Cavalcanti,<sup>a</sup> Luiz H. S. Gasparotto,<sup>a</sup> Edgar P. Moraes<sup>a</sup> and Fabrício G. Menezes<sup>a\*</sup>

The development of nanoprobess for selective detection of metal ions in solution has attracted great attention due to their impact on living organisms. As a contribution to this field, this paper reports the synthesis of silver nanoparticles modified with rutin in the presence of ascorbic acid and their successful use as a chromogenic probe for the selective detection of Fe<sup>3+</sup> in aqueous solution. Limits of detection and quantification were found to be 17 nmol L<sup>-1</sup> and 56 nmol L<sup>-1</sup>, respectively. The sensing ability is proposed to proceed *via* an iron-induced nanoparticle growth/aggregation mechanism. A practical approach using image analysis for quantification of Fe<sup>3+</sup> is also described.

Received 23rd August 2019  
 Accepted 16th September 2019

DOI: 10.1039/c9ra06653e

[rsc.li/rsc-advances](http://rsc.li/rsc-advances)

Metal ions are key species in nature due to their essential functions in living organisms.<sup>1,2</sup> On the other hand, heavy metals as well as essential metals at abnormally high levels are toxic.<sup>2</sup> Iron, for instance, in addition to its popular use in industry and construction, is essential to the human body and active in biological processes. Although the trivalent form of iron is particularly important for oxygen transport in blood and the mitochondrial respiratory chain, high levels of this cation are associated with important pathologies.<sup>3,4</sup> The detection of metal ions in aqueous solution is traditionally performed by methods including atomic absorption spectrometry,<sup>5</sup> electrochemical measurements,<sup>6,7</sup> and inductively coupled plasma techniques,<sup>8</sup> among others. However, these techniques have important drawbacks, notably the need for sophisticated instrumentation, in addition to being time-consuming and requiring laborious procedures. To overcome these issues, the development of chromogenic and fluorogenic chemosensors for the selective detection of metal-targets has attracted great attention, especially due to the possibility of fast, sensitive and non-expensive analysis.<sup>9,10</sup> In the last decade, nanoscaled materials have been reported as selective probes for metal ions, including Fe<sup>3+</sup>.<sup>11–24</sup>

Silver nanoparticles (AgNPs) are of particular interest because of the affordable price of starting materials, ease of controlling size and morphology, possibility to functionalize

their surface with organic molecules, and optical properties that enable detection of a variety of analytes *via* simple UV-vis spectroscopy and digital image analysis. Furthermore, applications of AgNPs are also biotechnologically relevant due to the possibility of green synthetic protocols, including the use of plant extracts,<sup>25</sup> natural sources,<sup>26</sup> glycerol,<sup>27</sup> among others.

Flavonoids are secondary metabolites naturally found in fruits and other vegetables with relevant roles due to their nutritional, pharmaceutical and medicinal properties.<sup>28</sup> Because of their adequate structural features, flavonoids are candidates to be employed in the synthesis of AgNPs.<sup>26</sup> Rutin (RU), a sugar-based flavonoid, may be employed as reducing agent in the synthesis of AgNPs along with a stabilizer such as polyvinylpyrrolidone (PVP)<sup>26</sup> or used as crude plant extract component.<sup>29,30</sup>

This paper reports the use of RU-modified AgNPs (RU-AgNPs) as a chromogenic probe for Fe<sup>3+</sup> in aqueous medium in the presence of ascorbic acid (AA). Sensing ability of RU-AgNPs for the selective detection of Fe<sup>3+</sup> toward other metal cations was investigated with UV-vis spectroscopy analysis. These data and transmission electronic microscopy (TEM) results allowed a mechanistic proposal involved in the selective detection of Fe<sup>3+</sup> by RU-AgNPs. Furthermore, a practical approach based on correlation of images of solutions obtained with a conventional smartphone and chemometrics was employed for a simpler quantification of Fe<sup>3+</sup> in aqueous medium.

Initially, the order of reagent combination was investigated in the synthesis of RU-AgNPs. Concentration of RU ranged from 0.10 to 0.50 mmol L<sup>-1</sup>, while concentrations of other components were fixed at 0.20 mmol L<sup>-1</sup> AgNO<sub>3</sub>, 0.10 mmol L<sup>-1</sup> AA

<sup>a</sup>Institute of Chemistry, Federal University of Rio Grande do Norte, Natal, 59072-970, RN, Brazil. E-mail: fgenezes10@gmail.com

<sup>b</sup>Department of Chemistry, Federal University of Santa Catarina, Florianópolis, 88040-900, SC, Brazil

† Electronic supplementary information (ESI) available. See DOI: 10.1039/c9ra06653e



and 0.10 M NaOH. Water was used as solvent in all cases. Narrower surface plasmon resonance (SPR) bands were obtained from adding a solution of AA and NaOH to a solution containing RU and AgNO<sub>3</sub> (Fig. 1a) against the addition of RU, AA, and NaOH to AgNO<sub>3</sub> solution (Fig. S1a – ESI†), or the addition of RU and NaOH to a solution of AA and AgNO<sub>3</sub> (Fig. S1b†). RU-AgNPs obtained from the condition presented in Fig. 1a are small (4.1 nm average diameter) and considerably polydisperse (standard deviation of 4.7 nm), however, presenting only one population (Fig. 1b and S2†). A study of the influence of RU concentration (0.10 to 0.50 mmol L<sup>-1</sup>) on the stability of RU-AgNPs over time indicated that 0.10 mmol L<sup>-1</sup> RU generates more stable RU-AgNPs (Fig. S3†). Next, a study on the influence of pH indicated that RU-AgNPs are only stable under strong alkaline conditions (pH 12.5 or higher) (Fig. S4†).

The ability of RU-AgNPs to sense metal cations was investigated by both naked-eye and UV-vis spectroscopy analysis (Fig. 2). The separate addition of 10 μmol L<sup>-1</sup> of several metal cations (Fe<sup>3+</sup>, Co<sup>2+</sup>, Zn<sup>2+</sup>, Sr<sup>2+</sup>, Cu<sup>2+</sup>, Al<sup>3+</sup>, Ba<sup>2+</sup>, Cd<sup>2+</sup>, Pb<sup>2+</sup>, Ni<sup>2+</sup>, Mg<sup>2+</sup>, Hg<sup>2+</sup>, Cu<sup>+</sup> and Cr<sup>3+</sup>) to solutions of RU-AgNPs (prepared according to Fig. 1a) indicated that only Fe<sup>3+</sup> induces a significant colorimetric change in the final aspect of solution after 50 minutes (Fig. 2a).

The results presented in Fig. 2a are consistent with the UV-vis spectroscopy analysis (Fig. 2b). Co<sup>2+</sup> ions also induce some change in the system, however at a considerably smaller extension than Fe<sup>3+</sup>. In this study, AA played a crucial role in the selective detection of Fe<sup>3+</sup> by the referred nanoprobe. In the absence of AA, Co<sup>2+</sup> (mainly) as well as other cations induce stronger colorimetric and spectral changes (Fig. S5a and b,† respectively) in the analysis of solutions of RU-AgNPs when compared to the system containing AA. This selectivity may arise from two possible reasons: (i) preservation of RU by avoiding its oxidation in the reduction of Ag<sup>+</sup> ions; (ii) coordination of ascorbate anion to cations other than Fe<sup>3+</sup>.

Interaction of RU-AgNPs and Fe<sup>3+</sup> (10 μmol L<sup>-1</sup>) stabilizes after approximately 40 minutes (Fig. S6†). Next, a calibration curve was built from the direct relationship between the absorbance at 396 nm and the concentration of Fe<sup>3+</sup> (Fig. 2c), presenting a good correlation ( $R^2 = 0.9929$ ). The limits of detection and quantification were found to be 17 nmol L<sup>-1</sup> and 56 nmol L<sup>-1</sup>, respectively, which is very satisfactory.<sup>13,14</sup> The

influence of other cations in the detection of Fe<sup>3+</sup> was investigated by UV-vis spectroscopy. Fig. S7† clearly demonstrates that there are only small changes when a second cation (30 μmol L<sup>-1</sup>) is added together with Fe<sup>3+</sup> to the RU-AgNPs solution.

Mechanistically, the detection of Fe<sup>3+</sup> by RU-AgNPs in aqueous medium proceeds *via* a growth/aggregation-combined process. This proposal is first evidenced by UV-vis analysis due the suppression of SPR band (Fig. 2b), a behavior consistent with the literature.<sup>31,32</sup> Interestingly, TEM analysis clearly shows a growth in AgNPs size after addition of Fe<sup>3+</sup> to the solution (Fig. 2d), resulting in a final single AgNPs population with average diameter of 14.7 nm ± 8.9 nm. Due to the strong alkaline medium, the main specie responsible for the behavior of NPs is likely to be Fe(OH)<sub>3</sub>. A schematic illustration of the mechanism involving aggregation of RU-AgNPs induced by the addition of Fe<sup>3+</sup> is presented in Fig. 3. AgNPs are initially formed by adsorption of anionic RU to the silver surface *via* deprotonated 5-hydroxychromen-4-one moiety. This is supported by the literature<sup>33</sup> and confirmed by alteration in the 1800–1500 cm<sup>-1</sup> region of the RU infrared spectra before and after coordination with silver (Fig. S9†). Afterwards, the addition of Fe<sup>3+</sup> induces the formation of a coordination complex through an anionic catechol group, in which at least 2 : 1 ligand-Fe<sup>3+</sup> stoichiometry is required for an aggregated effect.

Due to increasing interest in image processing as an analytical tool for many purposes,<sup>34,35</sup> Multiple Linear Regression was employed to verify the capacity of the RU-AgNPs to probe Fe<sup>3+</sup> standards at distinct concentrations, as presented in Fig. 4. The curve was obtained by plotting the color absorbances RGB-based values *versus* the concentrations of Fe<sup>3+</sup> standards after RU-AgNPs interaction. Predicted iron is a vector based on RGB values that were then extracted from the filtered images and inserted in the equation described by Beer-Lambert law in order to generate the absorbances for the construction of the analytical curve. A linear behavior between the predicted response and the measured concentrations was observed ( $R^2 = 0.9806$ ).

Regression coefficients of the calibration model (using the R, G and B channels simultaneously) obtained by MLR method are shown in eqn (1):

$$[\text{Fe}^{3+}] = 44.5R - 4.9G - 16.4B + 5.1 \quad (1)$$

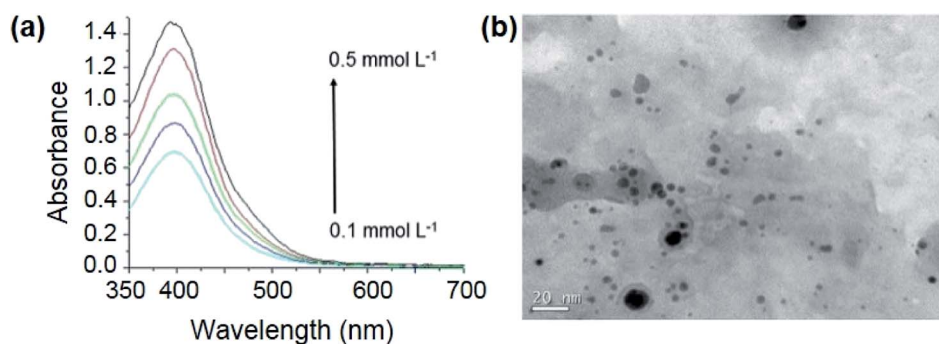


Fig. 1 (a) UV-vis analysis of RU-AgNPs under strong alkaline condition (pH > 12.5) based on the order of adding reagents (RU, 0.10 to 0.50 mmol L<sup>-1</sup>; AgNO<sub>3</sub>, 0.20 mmol L<sup>-1</sup>; AA, 0.10 mmol L<sup>-1</sup>; NaOH, 0.10 mmol L<sup>-1</sup>); (b) TEM image of RU-AgNPs under the selected condition.



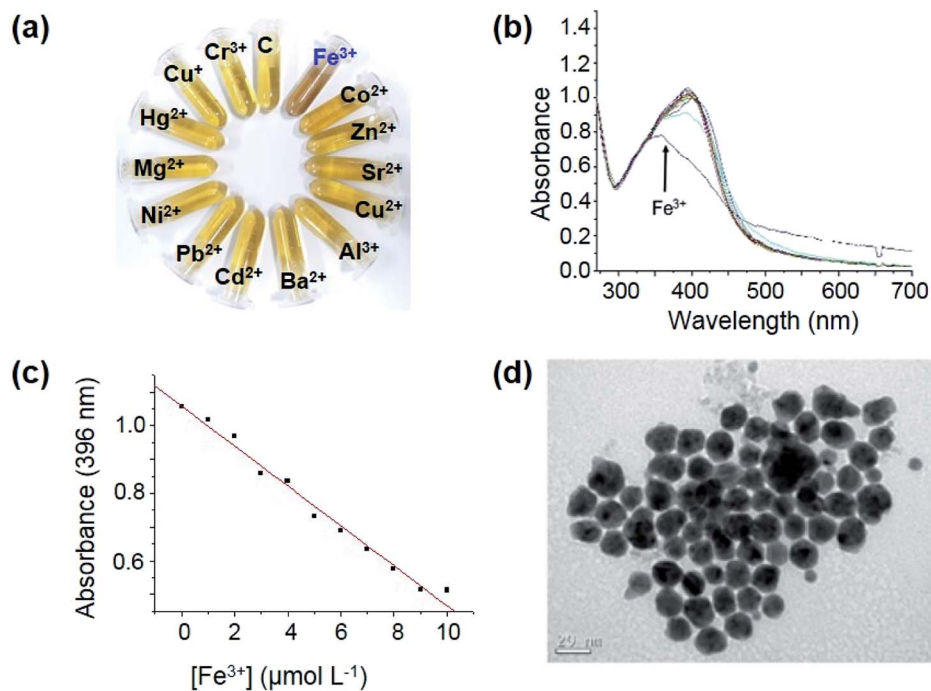


Fig. 2 Naked-eye (a) and UV-vis (b) analysis of RU-AgNPs in absence (control, C) and presence of  $10 \mu\text{mol L}^{-1}$  of selected metal cations ( $\text{Fe}^{3+}$ ,  $\text{Co}^{2+}$ ,  $\text{Zn}^{2+}$ ,  $\text{Sr}^{2+}$ ,  $\text{Cu}^{2+}$ ,  $\text{Al}^{3+}$ ,  $\text{Ba}^{2+}$ ,  $\text{Cd}^{2+}$ ,  $\text{Pb}^{2+}$ ,  $\text{Ni}^{2+}$ ,  $\text{Mg}^{2+}$ ,  $\text{Hg}^{2+}$ ,  $\text{Cu}^{+}$  and  $\text{Cr}^{3+}$ ) after 50 min; (c) calibration curve obtained by the addition of different amounts (0 to  $10 \mu\text{mol L}^{-1}$ ) of  $\text{Fe}^{3+}$  to solutions of RU-AgNPs; (d) TEM image of RU-AgNPs after addition of  $\text{Fe}^{3+}$  ( $10 \mu\text{mol L}^{-1}$ ). In all experiments, RU-AgNPs were prepared in the presence of ascorbic acid.

where  $\text{Fe}^{3+}$  concentration is the dependent variable (Predicted Iron), 5.1 is the intercept ( $\beta_0$ ), 44.5,  $-4.9$  and  $-16.4$  are the regression coefficients of the independent variables (R, G and B channels, respectively).

It is possible to observe an interesting performance of the method using the three RGB color channels allied with MLR to quantify the  $\text{Fe}^{3+}$  content, which presented reasonable deviations in its responses considering that it is simple and low-cost. The good linearity is similar to other colorimetric methods such as sodium determination in seawater and coconut water ( $R^2 > 0.91$ ) by Moraes and coauthors,<sup>36</sup> or iron(II) in simulated seawater ( $R^2 = 0.9993$ ) by Gasparotto *et al.*<sup>37</sup>

Second order regression was applied to the dataset to obtain a better adjustment, resulting in an adjusted  $R$ -squared of 0.9955. RGB values were then inserted in eqn (2) in order to generate the construction of the correlation:

$$[\text{Fe}^{3+}] = 14.4R + 30.7G - 23.4B - 398RG - 348RB - 0.8BG - 978R^2 + 695G^2 + 26.9B^2 + 4.5 \quad (2)$$

This paper reports the use of AgNPs functionalized with RU as nanoprobes for selective detection and sensitive quantification of  $\text{Fe}^{3+}$  in aqueous solution. The synthesis of RU-AgNPs is reproducible, easily performed and requires no stabilizer agent

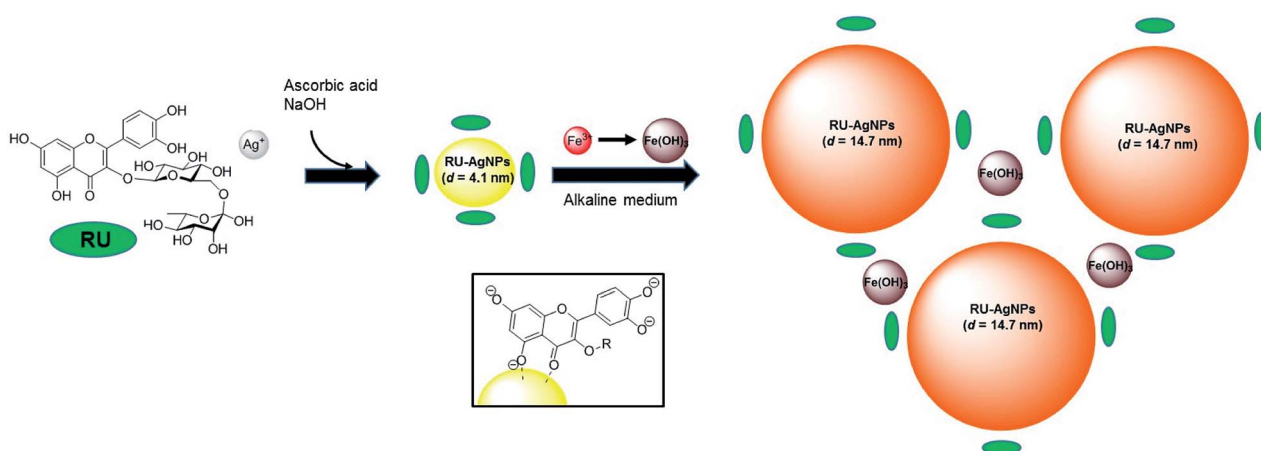


Fig. 3 Mechanistic proposal for growth/aggregation of RU-AgNPs in the presence of  $\text{Fe}^{3+}$ . Insert: binding model for RU-AgNPs.



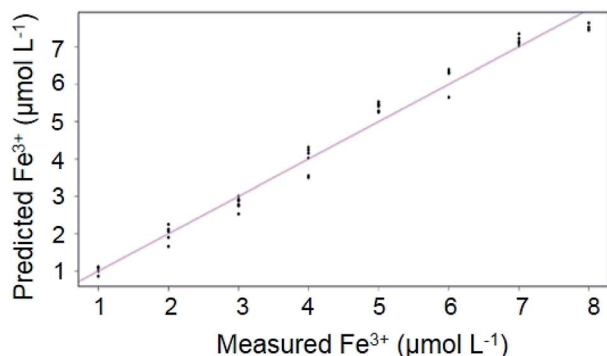


Fig. 4 Calibration curve for  $\text{Fe}^{3+}$  analysis showing the predicted iron (RGB) vs. iron(III) concentration (1 to  $8 \mu\text{mol L}^{-1}$ ). Adjusted  $R^2 = 0.9806$ .

other than RU. AA has a crucial role in the selectivity by either the avoidance of oxidation of RU by silver and/or coordination of ascorbate with other cations. The literature brings relevant examples of chromogenic and fluorogenic chemosensors for selective detection of  $\text{Fe}^{3+}$  in solution. Many of these artificial organic receptors present high selectivity and relevant limits of detection, requiring, however, very specific reagents and laborious synthetic procedures.<sup>38–41</sup> Metal-based nanoparticles have emerged as potential probes for detection of  $\text{Fe}^{3+}$ .<sup>11–16</sup> Although effective in  $\text{Fe}^{3+}$  sensing, the synthesis of these nanoprobe require some toxic reagents, such as  $\text{NaBH}_4$  or PVP, use plant extracts, which may lead to some drawbacks, such as the understanding of the sensing mechanism. In contrast, our method is based on commercially available, nontoxic, low-cost reagents.  $\text{Fe}^{3+}$  sensing performed satisfactorily in the  $1\text{--}10 \mu\text{mol L}^{-1}$  range, and the limit of detection obtained with this method ( $17 \text{ nmol L}^{-1}$ ) is comparable to the most sensitive methods reported in literature. A mechanism for the detection of  $\text{Fe}^{3+}$  by RU-AgNPs involves a combined growth/aggregation of the NPs. There is a still limited number of nanoscaled systems reported as being selective and sensitive in the detection of  $\text{Fe}^{3+}$ , which reinforces the relevance of the method reported herein. The linearity range obtained by both UV-vis spectroscopy and image analysis comprises the maximum of residual  $\text{Fe}^{3+}$  in drinking water according to the European and US legislations.<sup>15,42</sup>

## Conflicts of interest

There are no conflicts to declare.

## Acknowledgements

The authors thank the Brazilian entities Conselho Nacional de Pesquisa e Desenvolvimento (CNPq), Conselho de Aperfeiçoamento de Pessoal de Nível Superior (CAPES – Finance code 001) and Financiadora de estudos e Projetos (FINEP) for financial support. This work was also supported by the Central Laboratory of Electron Microscopy (LCME) at UFSC.

## Notes and references

- M. Ahmed, M. Faisal, A. Ihsan and M. M. Naseer, *Analyst*, 2019, **144**, 2480.
- J. Zhang, F. Cheng, J. Li, J. J. Zhu and Y. Lu, *Nano Today*, 2016, **11**, 309.
- T. Wei, J. Liu, H. Yao, Q. Lin, Y. Xie, B. Shi, P. Zhang, X. You and Y. Zhang, *Chin. J. Chem.*, 2013, **31**, 515.
- N. Abbaspour, R. Hurrell and R. Kelishadi, *J. Res. Med. Sci.*, 2014, **19**, 164.
- B. Welz, M. G. R. Vale, É. R. Pereira, I. N. B. Castilho and M. B. Dessuy, *J. Braz. Chem. Soc.*, 2014, **25**, 799.
- M. Lu, N. V. Rees, A. S. Kabakaev and R. G. Compton, *Electroanalysis*, 2012, **24**, 1693.
- M. Sander, T. B. Hofstetter and C. A. Gorski, *Environ. Sci. Technol.*, 2015, **49**, 5862.
- L. Poirier, J. Nelson, D. Leong, L. Berhane, P. Hajdu and F. Lopez-linares, *Energy Fuels*, 2016, **30**, 3783.
- D. T. Quang and J. S. Kim, *Chem. Rev.*, 2010, **110**, 6280.
- H. Zhu, J. Fan, B. Wang and X. Peng, *Chem. Soc. Rev.*, 2015, **44**, 4337.
- S. Ghosh, S. Maji and A. Mondal, *Colloids Surf., A*, 2018, **555**, 324.
- A. Jain, S. Wadhawan, V. Kumar and S. K. Mehta, *Chem. Phys. Lett.*, 2018, **706**, 53.
- S. S. Memon, A. Nafady, A. R. Solangi, A. M. Al-Enizi, Sirajuddin, M. R. Shah, S. T. H. Sherazi, S. Memon, M. Arain, M. I. Abro and M. I. Khattak, *Sens. Actuators, B*, 2018, **259**, 1006.
- S. P. Wu, Y. P. Chen and Y. M. Sung, *Analyst*, 2011, **136**, 1887.
- J. Li, Q. Wang, Z. Guo, H. Ma, Y. Zhang, B. Wang and D. Bin, *Sci. Rep.*, 2016, **6**(1), 23558.
- B. A. Makwana, D. J. Vyas, K. D. Bhatt, V. K. Jain and Y. K. Agrawal, *Spectrochim. Acta, Part A*, 2015, **134**, 73.
- Z. Du, B. Song, W. Zhang, C. Duan, Y. Wang, C. Liu, R. Zhang and J. Yuan, *Angew. Chem., Int. Ed.*, 2018, **57**, 3999.
- H. Jia, X. Gao, Y. Shi, N. Sayyadi, Z. Zhang, Q. Zhao, Q. Meng and R. Zhang, *Spectrochim. Acta, Part A*, 2015, **149**, 674.
- H. Feng, Z. Zhang, Q. Meng, H. Jia, Y. Wang and R. Zhang, *Adv. Sci.*, 2018, **5**, 1800397.
- H. Feng, Y. Wang, J. Liu, Z. Zhang, X. Yang, R. Chen, Q. Meng and R. Zhang, *J. Mater. Chem. B*, 2019, **7**, 3909.
- H. Feng, Q. Meng, Y. Wang, C. Duan, C. Wang, H. Jia, Z. Zhang and R. Zhang, *Chem.-Asian J.*, 2018, **13**, 2611.
- Y. Jiao, J. Yin, H. He, X. Peng, Q. Gao and C. Duan, *J. Am. Chem. Soc.*, 2018, **140**, 5882.
- Y. Wang, R. Song, K. Guo, Q. Meng, R. Zhang, X. Kong and Z. Zhang, *Dalton Trans.*, 2016, **45**, 16616.
- Q. Han, J. Liu, Q. Meng, Y. Wang, H. Feng, Z. Zhang, Z. P. Xu and R. Zhang, *ACS Sens.*, 2019, **4**, 309.
- A. Roy, O. Bulut, S. Some, A. K. Mandal and M. D. Yilmaz, *RSC Adv.*, 2019, **9**, 2673.
- E. A. Terenteva, V. V. Apyari, S. G. Dmitrienko and Y. A. Zolotov, *Spectrochim. Acta, Part A*, 2015, **151**, 89.



- 27 A. G. Garcia, P. P. Lopes, J. F. Gomes, C. Pires, E. B. Ferreira, R. G. M. Lucena, L. H. S. Gasparotto and G. Tremiliosi-Filho, *New J. Chem.*, 2014, **38**, 2865.
- 28 M. L. Ferreyra, S. P. Rius and P. Casati, *Front. Plant Sci.*, 2012, **3**, 1.
- 29 S. Jain and M. S. Mehata, *Sci. Rep.*, 2017, **7**, 15867.
- 30 A. Im, L. Han, E. R. Kim, J. Kim, Y. S. Kim and Y. Park, *Phytother. Res.*, 2012, **26**, 1249.
- 31 Y. Bhattacharjee, D. Chatterjee and A. Chakraborty, *Sens. Actuators, B*, 2018, **255**, 210.
- 32 S. Manivannan, Y. Seo, D. Kang and K. Kim, *New J. Chem.*, 2018, **42**, 2007.
- 33 Y. He, F. Wei, Z. Ma, H. Zhang, Q. Yang, B. Yao, Z. Huang, J. Li, C. Zeng and Q. Zhang, *RSC Adv.*, 2017, **7**, 39842.
- 34 L. C. da Silva, D. F. de Lima, J. A. Silva, C. L. M. de Morais, B. L. Albuquerque, A. J. Bortoluzzi, J. B. Domingos, R. M. Araújo, F. G. Menezes and K. M. G. Lima, *J. Braz. Chem. Soc.*, 2016, **27**, 1077.
- 35 C. L. M. Morais, A. C. O. Neves, F. G. Menezes and K. M. G. Lima, *Anal. Methods*, 2016, **8**, 6458.
- 36 E. P. Moraes, N. S. A. da Silva, C. L. M. de Morais, L. S. das Neves and K. M. G. Lima, *J. Chem. Educ.*, 2014, **91**, 1958.
- 37 E. P. Moraes, M. R. Confessor and L. H. S. Gasparotto, *J. Chem. Educ.*, 2015, **92**, 1696.
- 38 Z. Li, Y. Zhou, K. Yin, Z. Yu, Y. Li and J. Ren, *Dyes Pigm.*, 2015, **105**, 7.
- 39 X. Han, D. Wang, S. Chen, L. Zhang, Y. Guo and J. Wang, *Anal. Methods*, 2015, **7**, 4231.
- 40 H. Jia, X. Gao, Y. Shi, N. Sayyadi, Z. Zhang, Q. Zhao, Q. Meng and R. Zhang, *Spectrochim. Acta, Part A*, 2015, **149**, 674.
- 41 N. Sharma, S. I. Reja, N. Gupta, V. Bhalla, D. Kaur, S. Arora and M. Kumar, *Org. Biomol. Chem.*, 2017, **15**, 1006.
- 42 A. J. Boguniewicz-Zablocka, I. Klosok-Bazan and V. Naddeo, *Environ. Sci. Pollut. Res.*, 2019, **26**, 1208.

